Social traits from stochastic paths in the core affect space

Giuseppe Boccignone*
Dipartimento di Informatica
Università degli Studi di Milano,
Milano, Italy
giuseppe.boccignone@unimi.it

Vittorio Cuculo*
Dipartimento di Informatica
Università degli Studi di Milano,
Milano, Italy
vittorio.cuculo@unimi.it

Alessandro D'Amelio*
Dipartimento di Informatica
Università degli Studi di Milano,
Milano, Italy
alessandro.damelio@unimi.it

Raffaella Lanzarotti*
Dipartimento di Informatica
Università degli Studi di Milano,
Milano, Italy
raffaella.lanzarotti@unimi.it

ABSTRACT

We discuss a preliminary investigation on the feasibility of inferring traits of social participation from the observable behaviour of individuals involved in dyadic interactions. Trait inference relies on a stochastic model of the dynamics occurring in the individual core affect state-space. Results obtained on a publicly available interaction dataset are presented and examined.

CCS CONCEPTS

• **Human-centered computing → HCI theory, concepts and models**.

KEYWORDS

HCI, social behaviour, affective computing, emotions, prediction

ACM Reference Format:
Giuseppe Boccignone, Vittorio Cuculo, Alessandro D'Amelio, and Raffaella Lanzarotti. 2019. Social traits from stochastic paths in the core affect space. In *The 13th International Conference on Pervasive Computing Technologies for Healthcare (PervasiveHealth'19), May 20–23, 2019, Trento, Italy.* ACM, New York, NY, USA, 6 pages. https://doi.org/10.1145/3329189.3329220

1 INTRODUCTION

Psychological well-being is intricately tied to changes of feeling [15]. Meanwhile, feeling dynamics impacts on how we act (and vice versa), interpersonal behaviour being no exception.

Under such circumstances, it is tempting to investigate whether and to which extent the connection between covert states of affect of individuals and their overt social behaviour can be computationally exploited for inferential purposes. This is the chief research question we address in this note.

Indeed answering such question can be important in prospect beyond its theoretical interest. One such case is the automated monitoring and intervention tools in healthcare and well-being, e.g. systems that assess motivation or engagement to the therapeutic program, or promote them through the interaction of subjects with social agents either virtual or real [32].

Among the several kinds of social behaviour, here we focus on social participation. Social participation is an important health determinant: for example, it is considered a key factor in successful aging. Overall, it is an emerging intervention goal of health professionals such as psychologists, sociologists, and gerontologists (but see [18] for an in-depth discussion).

In what follows we proceed by first introducing a stochastic model of the fluctuations of individual's affect (Section 2). The model stems from a tradition of work on random walks in biology [6], and builds further on more recent analyses [17] that introduced the Ornstein-Uhlenbeck (OU) process in the psychology of affect. The OU process has shown to offer a reasonable and explainable description of the dynamics of core affect variation. Surprisingly, to the best of our knowledge, this kind of approach has hitherto been overlooked in the context of computing technologies in healthcare and well-being.

Further, in the psychological field such stochastic models have been employed to handle data from experience sampling studies collected over days. Differently, here we exploit raters' continuously labelled data of relatively brief interactions as provided by the RECOLA dataset [25]. RECOLA is a well-known public multimodal corpus designed to monitor subjects as they worked in pairs remotely to complete a collaborative task (dyadic interactions). This corpus suits our needs, because doing an activity with others - namely, collaborating to reach the same goal - is a central level of involvement of the individual with others [18]. Most important for the work described here, the data are manually annotated with either the continuous core affect labels of arousal/valence and the participation levels.

On such basis, the OU model parameters are inferred in a realistic dyadic interaction setting (Section 3). From then on we investigate the predictive capability of the model, namely of its parameters, with respect to dimensions characterising the social participation of human subjects. Some preliminary conclusions are drawn in Section 4.

*All authors contributed equally to this research.

PervasiveHealth'19, May 20–23, 2019, Trento, Italy

ACM ISBN 978-1-4503-6126-2/19/05…$15.00
https://doi.org/10.1145/3329189.3329220

2 MODELLING AFFECT FLUCTUATIONS

Moment-by-moment, the covert emotional state of a person can be summarised, at the psychological level, in terms of how pleasant or unpleasant (valence, V) and how activated (arousal, A) the person is [1, 26]. By and large, fluctuations of affect reflect how we deal with variations in the environment and how we regulate our emotions. Cogently, a variety of studies, e.g. [4, 28], provide evidence of the connection between the covert core affect and the dimensions characterising individual's overt interpersonal behaviour.

At the neurobiological level, core affect dynamics is consequent on the activity of a complex, open system. The latter is more suitably conceived as subject to stochastic variability resulting from the entanglement of many internal (and external) activities that influence it [17]. Across time, the core affect unfolding, as observed from the sampling of experiential data, can be represented as a trajectory, i.e. a realisation of a stochastic process. Such random path reflects the typical pattern of affective changes and fluctuations that V/A levels undergo across time and that characterise an individual [17].

The dynamics of stochastic trajectories in the core affect manifold can be formalised as follows. On a measurable state-space $(\Omega, \mathcal{A}, \mathbb{P})$ define:

- a family of probability measures $\mathcal{M} = \{\mathbb{P}_\theta, \theta \in \Theta\}$ depending on a parameter θ, with density P_θ;
- a pair of stochastic processes $X = \{X_t, 0 \le t \le T\}$ and $Y = \{Y_t, 0 \le t \le T\}$ taking values in $\mathbb{R}_x$ and $\mathbb{R}_y$, respectively.

Suppose X, under $\mathbb{P}_\theta$, is a Markov process with an infinitesimal generator, then we can write the state-space equations of a dynamical stochastic system in the following form of Itô Stochastic Differential Equations (SDE, to be interpreted as an Itô stochastic integral):

$$dX_t = f(X_t, U_t)dt + D^{1/2}dW_t, \tag{1}$$

$$dY_t = g(X_t, U_t)dt + R^{1/2}dV_t, \tag{2}$$

where $W = \{W_t, 0 \le t \le T\}$ and $V = \{V_t, 0 \le t \le T\}$ are respectively independent standard processes (e.g. Wiener), of the same dimension of X and Y respectively. D, R are diffusion coefficients. The latter could be in general a function of the states, i.e. $D = D(X_t), R = R(X_t)$.

The variable U also is defined for wider generality as the stochastic process $U = \{U_t, 0 \le t \le T\}$, though in specific cases can be deterministic, stochastic, or both. It represents the system control, which is also variously referred to in the literature as input, cause or source. This can be shaped in many ways, for example as a function of both X and Y (e.g. to introduce feedback) or an exogenous input (e.g., the labelling sequence provided along a supervised learning stage).

Also, we denote f and g the generic (vector or scalar valued) nonlinear, potentially time-varying functions, i.e. mappings of the kind $T \times L^2(\Omega, \mathcal{A}, \mathbb{P}) \mapsto L^2(\Omega, \mathcal{A}, P)$ to a (Lebegue square-integrable) Hilbert space $L^2(\Omega, \mathcal{A}, P)$ with finite second-order moments.

In fact, Eqs. (1) and (2) can be easily recognised as diffusion processes, f and g being their respective drifts [30]. We can think of this processes as the limit of the discrete-time processes

$$X_{t+\Delta t} - X_t = f(X_t, U_t)\Delta t + D^{1/2}\sqrt{\Delta t}\epsilon_{X_t}, \tag{3}$$

$$Y_{t+\Delta t} - Y_t = g(X_t, U_t)\Delta t + R^{1/2}\sqrt{\Delta t}\epsilon_{Y_t}. \tag{4}$$

Equations (3) and (4) are known as the Euler-Maruyama approximation of Eqs (1) and (2), respectively.

Assume that Ω is the canonical state-space $\Gamma([0, T]; \mathbb{R}_{x+y})$, in which case X and Y are the canonical processes on $\Gamma([0, T]; \mathbb{R}_x)$ and $\Gamma([0, T]; \mathbb{R}_y)$, respectively, and P_θ is the probability law of (X, Y). In such case X is the state process, which is not directly observed; rather, the information about its evolution is obtained through the noisy observed process Y.

Then, Eqs. (1) and (2) define a generalised input-output state-space model (SSM) where the states X_t mediate the influence of the input on the output and endow the system with memory. The state and observation perturbations or fluctuations are provided by noise terms ϵ_X, ϵ_Y, which can be defined via the stochastic integrals $W_t = \int_0^t \epsilon_{X_s} ds$, $V_t = \int_0^t \epsilon_{Y_s} ds$. In the case of W, V being Wiener processes, ϵ_X, ϵ_Y represent Gaussian additive noise, and have the same dimension of X, Y, respectively. If errors are iid Gaussian random variables, then the specific scaling of the white noise with Δt gives rise to the nondifferentiable trajectories of sample paths characteristic for a diffusion process.

The classic input-output SSM can be recovered from Eqs. (1, 2), under the independence assumption $(Y_t \perp Y_{t-1} \mid X_t)$:

$$dX_t = f(X_t, U_t)dt + D^{1/2}dW_t, \tag{5}$$

$$Y_t = g(X_t, U_t) + R^{1/2}\epsilon_{Y_s}. \tag{6}$$

By setting $f(X_t, U_t) = B(U - X_t)$ and $g(X_t, U_t) = X_t$ in Eqs. (5,6) the model for temporal fluctuations in the core affect state over time studied by [22] is recovered,

$$dX_t = B(U - X_t)dt + D^{1/2}dW_t, \tag{7}$$

$$Y_t = X_t + R^{1/2}\epsilon_{Y_s}, \tag{8}$$

where B is a positive definite matrix of parameters and control vector U in the simplest case is assumed to be a constant, i.e. $U = const$, or time-varying in the most general case. The instantaneous change in X_t, that is, dX_t, depends on how far the current state X_t is from the point U. This control parameter is called a steady state or attractor. The state equation (7) can be easily recognised as a form of the Ornstein-Uhlenbeck (OU) process [29]; thus Eqs. (7) and (8) together represent an OU-based input-output SSM (OU-SSM),

The parameter matrix B controls the magnitude of the "attraction" effect and it is defined as

$$B = \begin{bmatrix} B_{AA} & B_{AV} \\ B_{VA} & B_{VV} \end{bmatrix} \tag{9}$$

B_{AA} and B_{VV} represent the drift of the process towards the home base in the arousal and valence dimension respectively, while the off-diagonal elements $B_{AV} = B_{VA} = \rho_B\sqrt{B_{AA}B_{VV}}$ encode the cross-correlation between drift in both dimensions. For high values of B_{AA} or B_{VV} the difference between the actual state and U_A or U_V respectively tends to be magnified; therefore a faster change will occur in the direction of U for that specific dimension. For high values of the cross-correlation an increasing value of the drift in one dimension will positively affect the drift in the other, producing

more curved trajectories towards the home base. Based on this property, the parameter is often called the dampening force or centralising tendency.

Interestingly, U acts as a set point that reflects the baseline functioning of the system, an affective "home base", which reflect the affective comfort zone of an individual, signalling that everything is normal. The attractor keeps the system in balance by pulling core affect back to its home base, creating an emergent coherence around it. It is surmised, the attractor strength reflects the regulatory processes that are installed to keep a person's core affect in check. The stochastic innovation term dW_t incorporates the multiple smaller and larger impacts that the core affect system undergoes at a given moment.

To sum up, these three key processes - affective home base, attractor strength and variability - are largely responsible for producing the countless number of ways people can display changes and fluctuations in their core affect [17].

3 USING THE MODEL FOR PREDICTING SOCIAL PARTICIPATION

The procedure we follow is straightforward. We consider the annotated V/A trajectories of the subject s as a realization $Y^{(s)}$ from Eq. (8). Denote $\mathbf{\Theta}^{(s)}$ the core affect parameters defining the OU-SSM related to subject s and $z_i^{(s)}$ is the i-th social participation dimension label. Then, the problem we are addressing is the mapping:

$$Y^{(s)} \rightarrow \mathbf{\Theta}^{(s)} \rightarrow z_i^{(s)}.$$

From now on, we will drop subject's index s unless needed.

3.1 Dataset and social cues considered

Differently from approaches in the psychological literature, here we exploit the public available dataset RECOLA [25], which is a multimodal corpus of spontaneous collaborative and affective interactions in French. Aiming at studying the impact of emotional feedback on teamwork quality and efficiency, 46 participants took part in the test where several multimodal data, i.e., audio, video and physiological signals (specifically, electrocardiogram ECG, and electrodermal activity EDA) were recorded continuously and synchronously. In addition to these biosignals, 6 annotators concentrated on the labelling of both the affective and social behaviours that were produced by participants during their collaboration. As to affective behaviour, emotion was measured continuously on the two dimensions of arousal (A) and valence (V).

As previously mentioned, here we focus on social participation, a relevant facet of social behaviour. Participation dimensions considered in RECOLA are: agreement, dominance, engagement, performance and rapport. These have been selected based on various studies in the literature [25]. Social dimensions were rated once after having performed the annotation of the affective behaviours, using a 7-Likert scale. To such end a list of definitions and questions to the annotators was provided for each primitive:

1) *agreement*: does the person seem to agree with his/her partner?
2) *dominance*: does the person appear to be dominant?
3) *engagement*: does the person seem to be engaged?
4) *performance*: does the persons speech appear to be clear and relevant for the task?
5) *rapport*: does the person and his/her partner seem to be or could become friends?

3.2 Model learning

In order to fit the proposed model to the V/A trajectories, we adopt a Bayesian inference procedure based on Markov chain Monte Carlo (MCMC) sampling for the estimation of the model parameters.

Relying on the Euler-Maruyama discretization scheme (Eqs.3 and 4) and exploiting the Markov property of the OU process, the probability of the observed trajectory, given the parameters $\mathbf{\Theta} = \{U, B, D, R\}$ is:

$$P(Y|\mathbf{\Theta}) = \prod_{t=1}^{N-1} P(Y_{t+\Delta_t}|Y_t, \mathbf{\Theta}). \tag{10}$$

The posterior probability of the OU parameters given the sample trajectory follows from Bayes' theorem:

$$P(\mathbf{\Theta}|Y) = \frac{P(Y|\mathbf{\Theta})P(\mathbf{\Theta})}{P(Y)}. \tag{11}$$

In order to ensure the matrices B and D to be covariance matrices, we place LKJ priors [19] on them and an informative Gaussian prior for the U vector. The matrix R is assumed to be diagonal (i.e., uncorrelated errors for the two dimensions). The posterior distribution is then approximated by resorting to Hamiltonian Monte Carlo Sampling [12]. For each subject the convergence check of the MCMC algorithm is carried out by computing the Gelman-Rubin diagnostic, which compares the variance within a single chain to variance between chains with independent restarts [3], and ensuring that this value is no larger than 1.

3.3 Model checking

To assess whether the model can reproduce the patterns observed in the real data, we exploited the learned posterior distributions of the parameters $\mathbf{\Theta}$ for the generation of 100 V/A trajectories for each of the 23 subjects of RECOLA dataset. This approach, known as posterior predictive check (PPC) [10], consists in generating data from the model using parameters drawn from the posterior in order to analyze how good is the approximation of the underlying distribution. Fig. 1 depicts at a glance qualitative results. The first column of the left panel shows the actual core affect trajectories from subjects P17 and P37, whilst the remaining columns present two generations adopting the person-specific inferred parameters in the Eq. (8). The right panel shows the corresponding 2D spatial histograms, that is the empirical approximation of the spatial point process distribution induced by the stochastic walk over sites (bins) in the V/A state-space. Clearly, person-dependent parameters should allow to generate affective trajectories and related 2D spatial distributions consistent with actual subject data.

To quantitatively check the model, we calculated the 2D correlation coefficient between the 2D histogram of the observed data and the 2D histogram from simulated trajectories. When considering the core affect space as partitioned by three levels (low, neutral, high) for each affective dimension, we obtain nine possible area of interest (histogram 2D bins); in such setting the average correlation per person was CC = 0.966 (σ = 0.06). By resorting to a finer-grained grid, as the one adopted in Fig. 1b, the correlation

Grid size	Mean CC	Grid size	Mean CC
3x3	0.966 ± 0.06	18x18	0.632 ± 0.15
6x6	0.85 ± 0.13	21x21	0.602 ± 0.15
9x9	0.779 ± 0.15	24x24	0.566 ± 0.15
12x12	0.722 ± 0.16	27x27	0.541 ± 0.14
15x15	0.678 ± 0.15	30x30	0.511 ± 0.14

Table 1: 2D correlation coefficients and standard deviation, between the 2D histograms of the observed data and the 2D histograms of corresponding simulations as the grid size changes.

decreases accordingly (CC=0.779, $\sigma = 0.15$). Table 1 reports the results of an extensive test on the influence of the considered grid size.

3.4 Model prediction and analysis: results

The learnt OU parameters associated to each subject of the database, deliver an accurate and succinct representation of the dynamics of the core affect. Such parameters are used as features for predicting social behaviour labels in a classical supervised learning problem setting. Two regression models are considered in the following: Bayesian Linear Regression (BLR) and Gaussian Process Regression (GPR). The input to both models is a vector of features built by joining the inferred parameters of the OU process (U, B, D), namely the vector $\mathbf{p}^{(s)} \in \mathbb{R}^L$ with $L = 8$ (recall that B and D are symmetric matrices) for each subject s:

$$\mathbf{p}^{(s)} = [U_A, U_V, B_{AA}, B_{AV}, B_{VV}, D_{AA}, D_{AV}, D_{VV}]. \quad (12)$$

Besides regression *per se*, these techniques allow for statistical investigation into the relationship between OU parameters and social behaviour labels.

3.4.1 Bayesian Linear Regression. The BLR assumes the dependent variables (social behaviour traits) to be normally distributed, their mean given by a linear predictor:

$$z_i^{(s)} = \mathbf{p}^{(s)}\beta_i + \epsilon \qquad \epsilon \sim \mathcal{N}(0, \sigma^2). \quad (13)$$

Here, $z_i^{(s)}$ is the i-th social participation dimension label, $\mathbf{p}_s \in \mathbb{R}^L$ is the vector of OU parameters inferred for the subject s; $\beta_i \in \mathbb{R}^L$ is the vector of regression coefficients to be estimated. The estimation is performed by computing the posterior probability distribution of the regression coefficients given the data,

$$P(\beta_i|\mathbf{z}_i, \mathbf{P}) = \frac{P(\mathbf{z}_i|\beta_i, \mathbf{P})P(\beta_i|\mathbf{P})}{P(\mathbf{z}_i|\mathbf{P})}; \quad (14)$$

here $\mathbf{z}_i$ is the vector of corresponding labels for the i-th social behaviour, and $\mathbf{P} \in \mathbb{R}^{S\times L}$ is the design matrix containing the L inferred parameters of the OU model as columns, and the S subjects as rows. Again, the posterior is obtained by MCMC sampling.

Prediction is then carried out via Eq. (13) on a test vector $\mathbf{p}^{test}$.

The distribution over parameters rather than point estimates, allows to quantify the uncertainty on the estimation. A method to summarize such uncertainty is to consider the interval of values that lies within the 95% of the estimated distribution. Such value is called *Highest Density Interval* (HDI) and can be used to assess the statistical significance of the correlation between specific dependent and independent variables [16]. In particular, if the 0 value lies outside the HDI of a given regression coefficient, than the zero can be "rejected" as a plausible value for describing the relationship between a given couple of OU parameter and social behaviour label (slope of the regression line for that dimension), and consequently, a statistically significant correlation exists. In Table 2 the regression coefficients whose HDI do not include the zero value are reported.

Coefficient	Description	Mean Post. Distrib.	95% HDI
Agreement			
$\beta_{Agr}[U_V]$	β associated to the home base for the Valence dimension	0.54	0.056 ÷ 1.03
Dominance			
$\beta_{Dom}[U_A]$	β associated to the home base for the Arousal dimension	0.56	0.14 ÷ 0.97
Engagement			
$\beta_{Eng}[U_A]$	β associated to the home base for the Arousal dimension	0.62	0.27 ÷ 0.98
$\beta_{Eng}[D_{AA}]$	β associated to the diffusion on the Arousal dimension	0.44	0.13 ÷ 0.73

Table 2: Bayesian Linear Regression Coefficients not containing zero value in the HDI of the posterior.

Main results can be summarised as follows. Higher *Agreement* scores correspond to an home base with higher valence V. The same proportionality holds for both the *Dominance* and *Engagement* traits with respect to the home base. Interestingly enough, people with high engagement tend to have an higher variability in the arousal dimension.

3.4.2 Gaussian Process Regression. The GPR relaxes the assumption of linearity between the dependent and independent variables by allowing the prediction function to be nonparametric. In particular, given a vector of features $\mathbf{p}^{(s)}$ and the corresponding label $z_i^{(s)}$, we assume $z_i^{(s)}$ to be generated from an unknown function $f(\mathbf{p}^{(s)})$ plus Gaussian noise ϵ:

$$z_i^{(s)} = f(\mathbf{p}^{(s)}) + \epsilon \qquad \epsilon \sim \mathcal{N}(0, \sigma^2). \quad (15)$$

The prior distribution on $f(\mathbf{p}^{(s)})$ is defined as a Gaussian Process:

$$f(\mathbf{p}^{(s)}) \sim \mathcal{GP}\big(m(\mathbf{p}^{(s)}), \mathbf{K}\big), \quad (16)$$

where $\mathbf{K} = \kappa(\mathbf{p}^{(s)}, \mathbf{p}^{(s')}; \gamma)$ is the Radial Basis Function kernel with Automatic Relevance Determination (ARD-RBF) defined as:

$$\kappa(\mathbf{p}^{(s)}, \mathbf{p}^{(s')}; \gamma) = \eta^2 exp\Big[-\frac{1}{2}\sum_{d=1}^{L}\Big(\frac{p_d^{(s)} - p_d^{(s')}}{w_d}\Big)^2\Big]. \quad (17)$$

Here $\gamma = \{\eta^2, w_1, ..., w_L\}$ is the set of hyper-parameters of the model and L is the dimensionality of the input. η^2 represents the deviation of the function from the mean, while the values $\mathbf{w} = \{w_1, ..., w_L\}$ represent the length scale of the function along the

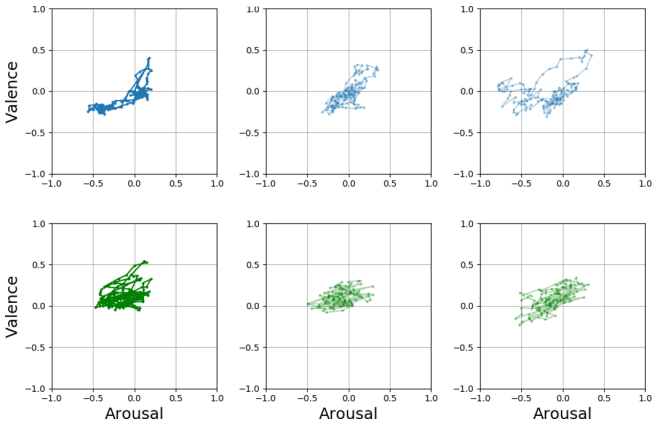

(a) Valence/arousal stochastic trajectories.

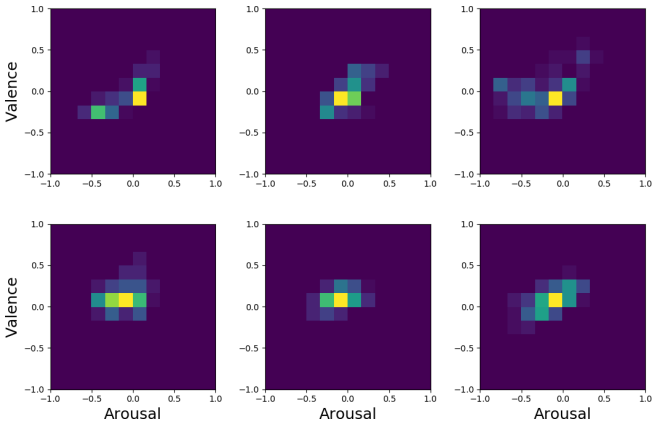

(b) 2D spatial histograms derived from trajectories in (a).

Figure 1: Observed and generated valence/arousal data. The first column of left (a) and right (b) panel refers to the observed data of subjects P17 (top) and P37 (bottom), respectively. In both panels, the following columns present data simulated from the OU state-space process relying on the inferred parameters, either in the form of raw stochastic V/A trajectories (a) and 2D histograms (b)

d dimension. For high length scale values in a particular dimension, the covariance becomes almost independent of that input, effectively removing it from the inference process [24]. As a consequence, the model is able to prune irrelevant dimensions, thus giving rise to an automatic determination of the structure of the regression model. The ARD weights, computed as $\eta^2/\mathbf{w}^2$, are automatically derived along the training procedure and provide an overview about the importance of each feature (OU parameter) for the regression/classification task, thus granting explainability and interpretability to the inferential step [7].

In Fig. 2 the learned ARD weights are depicted. It can be noted that the home base and the diffusion relative to the arousal dimension seems to be relevant for regressing the *Engagement* behaviour. The arousal home base is relevant for the *Dominance*, while the valence home base is relevant for the *Agreement*. These results are consistent with those obtained from BLR (Table 2). Meanwhile, it is worth noticing that although no statistically significant correlation was found in the BLR model between behaviour labels and the drift parameter of the OU model (B matrix), the GPR finds a strong relevance of such parameter for regressing the *Agreement* behaviour.

For both BLR and GPR the prediction has been carried out using a Leave-One-Out testing procedure: the models are learnt on the training set and tested on the held out example. The obtained prediction is compared to the true one by computing the RMSE. In Table 3 the average and standard deviation values of the RMSEs on the held out examples are reported for both models. Notably, the higher flexibility of the GPR produces slightly better results.

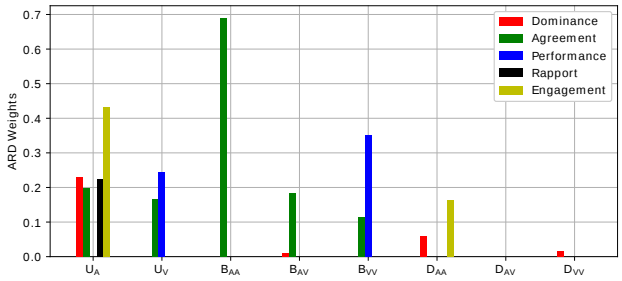

Figure 2: ARD weights after GPR training for the 5 social behaviour labels. On the x axis the OU parameters: Arousal home base (U_A), Valence home base (U_V), Drift in the V dimension (B_{VV}), Cross-correlation between drifts on the A and V dimension (B_{AV}), Drift in the A dimension (B_{VV}), Diffusion in the A dimension (D_{AA}), Cross-Correlation of the Diffusion on the A and V dimensions (D_{AV}), Diffusion on the V dimension (D_{VV}). On the y axis the ARD weight value learnt for each parameter.

4 DISCUSSION AND CONCLUSION

In this note we have explored the connection between covert states of affect of individuals, in terms of V/A dynamics, and their overt interpersonal behaviour, instantiated via social participation dimensions. In the vein of [17], the empirical V/A stochastic trajectories have been captured by an input-output OU-SSM. Such trajectories are likely to reflect the typical pattern of affective changes and fluctuations that characterises an individual [17]. To such end we have exploited the V/A time series that were collected in a public dataset as the empirical result of a human-based attribution (labelling) process. By and large this setting is akin to the setting that is likely to be handled when dealing with automated monitoring and intervention tools in healthcare and well-being. Meanwhile it differs from typical experimental setting adopted in studies in the psychology field, where participants are asked to monitor their core affect (or interpersonal behaviour) over days [17].

Yet, even in the setting considered here, results we have so far achieved suggest that stochastic modelling of core affect dynamics

Label	GPR	BLR
Dominance	0.56 ± 0.5	0.58 ± 0.38
Agreement	0.5 ± 0.4	0.49 ± 0.34
Performance	0.6 ± 0.52	0.72 ± 0.6
Rapport	0.9 ± 0.4	0.62 ± 0.54
Engagement	0.4 ± 0.28	0.49 ± 0.29

Table 3: Prediction results using Gaussian Process Regression (GPR) and Bayesian Linear Regression (BLR). Average RMSEs and standard deviation on the held out examples are reported.

highlights interesting relationships between parameters of stochastic variability in the core affect and social participation indexes.

In this preliminary inquiry we have straightforwardly used the given V/A time series as the input to the inferential process. However, nothing prevents from inferring V/A trajectories from the subjects' measurable behaviour (either visible or not) and subsequently exploit the latter for social behaviour analysis. Indeed, in recent years researchers'interest has been increasingly attracted by the analysis of non-acted spontaneous emotions [8, 27]. Such effort naturally calls for the exploitation of a continuous dimensional space, because it is more suitable to frame the subtlety of complex emotions [23]. Thus, a number of techniques have been developed to such aim either in a classic end-to-end approach [8, 21, 23, 27] and in the framework of generative, simulation-based accounts [2, 9, 11, 13, 14, 31].

This research trend is clearly relevant for affect-based systems in healthcare and well-being, with special reference to robotics. For instance, the above mentioned techniques can help socially assistive robots to interpret affective human body language of the elderly and their physiologically monitoring during one-on-one assistive scenarios [5, 32]. This way a robot can utilize affect estimation information in order to determine its own appropriate responsive behaviours so to keep people engaged in a given activity. One simple albeit significant example is providing cognitive and social stimulation during meal-time scenarios [20].

ACKNOWLEDGMENTS

This work was part of the project n. 2018-0858 title "Stairway to elders: bridging space, time and emotions in their social environment for wellbeing" supported by Fondazione CARIPLO.

REFERENCES

[1] David J Anderson and Ralph Adolphs. 2014. A framework for studying emotions across species. *Cell* 157, 1 (2014), 187–200.
[2] G. Boccignone, D. Conte, V. Cuculo, A. D'Amelio, G. Grossi, and R. Lanzarotti. 2018. Deep Construction of an Affective Latent Space via Multimodal Enactment. *IEEE Transactions on Cognitive and Developmental Systems* 10, 4 (2018), 865–880.
[3] Stephen P Brooks and Andrew Gelman. 1998. General methods for monitoring convergence of iterative simulations. *Journal of computational and graphical statistics* 7, 4 (1998), 434–455.
[4] Dana R Carney and C Randall Colvin. 2010. The circumplex structure of affective social behavior. *Social Psychological and Personality Science* 1, 1 (2010), 73–80.
[5] Filippo Cavallo, Francesco Semeraro, Laura Fiorini, Gergely Magyar, Peter Sinčák, and Paolo Dario. 2018. Emotion Modelling for Social Robotics Applications: A Review. *Journal of Bionic Engineering* 15, 2 (2018), 185–203.
[6] Edward A Codling, Michael J Plank, and Simon Benhamou. 2008. Random walk models in biology. *Journal of the Royal Society Interface* 5, 25 (2008), 813–834.
[7] Vittorio Cuculo, Alessandro D'Amelio, Raffaella Lanzarotti, and Giuseppe Boccignone. 2018. Personality Gaze Patterns Unveiled via Automatic Relevance Determination. In *Software Technologies: Applications and Foundations*. Springer International Publishing, Cham, 171–184.
[8] Sidney K D'Mello and Jacqueline Kory. 2015. A review and meta-analysis of multimodal affect detection systems. *ACM Computing Surveys (CSUR)* 47, 3 (2015), 43.
[9] Vittorio Gallese, Christian Keysers, and Giacomo Rizzolatti. 2004. A unifying view of the basis of social cognition. *Trends in cognitive sciences* 8, 9 (2004), 396–403.
[10] Andrew Gelman, Hal S Stern, John B Carlin, David B Dunson, Aki Vehtari, and Donald B Rubin. 2013. *Bayesian data analysis*. Chapman and Hall/CRC.
[11] Alvin I Goldman and Chandra Sekhar Sripada. 2005. Simulationist models of face-based emotion recognition. *Cognition* 94, 3 (2005), 193–213.
[12] Matthew D Hoffman and Andrew Gelman. 2014. The No-U-turn sampler: adaptively setting path lengths in Hamiltonian Monte Carlo. *Journal of Machine Learning Research* 15, 1 (2014), 1593–1623.
[13] Takato Horii, Yukie Nagai, and Minoru Asada. 2016. Imitation of human expressions based on emotion estimation by mental simulation. *Paladyn, Journal of Behavioral Robotics* 7, 1 (2016).
[14] T. Horii, Y. Nagai, and M. Asada. 2018. Modeling Development of Multimodal Emotion Perception Guided by Tactile Dominance and Perceptual Improvement. *IEEE Transactions on Cognitive and Developmental Systems* 10, 3 (2018), 762–775.
[15] Marlies Houben, Wim Van Den Noortgate, and Peter Kuppens. 2015. The relation between short-term emotion dynamics and psychological well-being: A meta-analysis. *Psychological bulletin* 141, 4 (2015), 901.
[16] John K. Kruschke. 2010. *Doing Bayesian Data Analysis: A Tutorial with R and BUGS* (1st ed.). Academic Press, Inc., Orlando, FL, USA.
[17] Peter Kuppens, Zita Oravecz, and Francis Tuerlinckx. 2010. Feelings change: accounting for individual differences in the temporal dynamics of affect. *Journal of personality and social psychology* 99, 6 (2010), 1042.
[18] Mélanie Levasseur, Lucie Richard, Lise Gauvin, and Émilie Raymond. 2010. Inventory and analysis of definitions of social participation found in the aging literature: Proposed taxonomy of social activities. *Social Science and Medicine* 71, 12 (2010), 2141 – 2149.
[19] Daniel Lewandowski, Dorota Kurowicka, and Harry Joe. 2009. Generating random correlation matrices based on vines and extended onion method. *Journal of multivariate analysis* 100, 9 (2009), 1989–2001.
[20] D. McColl and G. Nejat. 2014. Determining the affective body language of older adults during socially assistive HRI. In *2014 IEEE/RSJ International Conference on Intelligent Robots and Systems*. 2633–2638. https://doi.org/10.1109/IROS.2014.6942922
[21] Mihalis A Nicolaou, Hatice Gunes, and Maja Pantic. 2011. Continuous prediction of spontaneous affect from multiple cues and modalities in valence-arousal space. *IEEE Transactions on Affective Computing* 2, 2 (2011), 92–105.
[22] Zita Oravecz, Francis Tuerlinckx, and Joachim Vandekerckhove. 2011. A hierarchical latent stochastic differential equation model for affective dynamics. *Psychological methods* 16, 4 (2011), 468.
[23] Soujanya Poria, Erik Cambria, Rajiv Bajpai, and Amir Hussain. 2017. A review of affective computing: From unimodal analysis to multimodal fusion. *Information Fusion* 37 (2017), 98–125.
[24] Carl Edward Rasmussen and Christopher KI Williams. 2006. *Gaussian processes for machine learning*. The MIT Press, Cambridge, MA, USA.
[25] Fabien Ringeval, Andreas Sonderegger, Juergen Sauer, and Denis Lalanne. 2013. Introducing the RECOLA multimodal corpus of remote collaborative and affective interactions. In *Proc. 10th IEEE Int. Conf. and Workshops on Automatic Face and Gesture Recognition*. IEEE, 1–8.
[26] J. A. Russell. 2003. Core affect and the psychological construction of emotion. *Psychological review* 110, 1 (2003), 145.
[27] Evangelos Sariyanidi, Hatice Gunes, and Andrea Cavallaro. 2015. Automatic analysis of facial affect: A survey of registration, representation, and recognition. *IEEE Transactions on Pattern Analysis and Machine Intelligence* 37, 6 (2015), 1113–1133.
[28] Tinneke Timmermans, Iven Van Mechelen, and Peter Kuppens. 2010. The relationship between individual differences in intraindividual variability in core affect and interpersonal behaviour. *European Journal of Personality* 24, 8 (2010), 623–638.
[29] George E Uhlenbeck and Leonard S Ornstein. 1930. On the theory of the Brownian motion. *Physical review* 36, 5 (1930), 823.
[30] NG Van Kampen. 2011. *Stochastic Processes in Physics and Chemistry*. Elsevier.
[31] J. Vitale, M-A. Williams, B. Johnston, and G. Boccignone. 2014. Affective facial expression processing via simulation: A probabilistic model. *Biologically Inspired Cognitive Architectures Journal* 10 (2014), 30–41.
[32] Eva Wiese, Giorgio Metta, and Agnieszka Wykowska. 2017. Robots As Intentional Agents: Using Neuroscientific Methods to Make Robots Appear More Social. *Frontiers in Psychology* 8 (2017), 1663.